

Simulation of Defect Detection Schemes for Wafer Inspection in VLSI Manufacturing

Aaron Swecker^a, Andrzej Strojwas^a, Xiaolei Li^a, and Ady Levy^b

^aDepartment of Electrical and Computer Engineering
Carnegie Mellon University
Pittsburgh, PA 15213-3890

^bKLA Instruments
San Jose, CA 95134

Abstract-- The detection of critical defects on modern VLSI wafers is a challenging and complex problem. Simulation of these critical defects allows for rapid characterization and optimization of in-line detection schemes. In this paper we introduce a 3-D electromagnetic field simulator (METRO 3-D) that calculates the scattering of light from wafer topographies. An approach that allows highly absorptive materials to be investigated is discussed for the three dimensional topography simulator. With this enhancement to the simulator, several defect studies were performed and the results of these studies illustrate the ability of the simulator to model wafer topographies and defects that occur in modern fab lines.

I. INTRODUCTION

The number of process steps needed to manufacture a state-of-the-art integrated circuit (IC) has been increasing dramatically, while the size of the critical dimension has been shrinking. This drives the need to detect smaller and smaller defects while the potential for these critical defects increases with process complexity. In addition, new processes such as chemical mechanical polishing (CMP) are becoming more popular which brings new challenges to in-line detection with new defect types, yield loss mechanisms and noise sources[1]. In order to quickly ramp a process to high yields and to sustain those yield levels during volume production, sophisticated detection of process contamination is critical and becoming more challenging.

Optical defect inspection of wafers between process steps using an in-line system (e.g., bare wafer scanners or digital image comparison tools) provides information to quickly determine if the process is in control. There are several methods of optimizing these detection schemes, including (1) inspecting wafers with known built-in defects, (2) inspecting actual production wafers, or (3) simulating the electromagnetic characteristics of wafer topographies using metrology simulators. Since it is necessary to test and compare several schemes to determine the optimal detection configuration, simulations in conjunction with experimental verifications allow for efficient optimization. Using simulations, several scenarios can be quickly evaluated and compared by altering parameters such as wavelength and numerical aperture. Additionally, the simulations can be compared with a smaller database of actual experiments to ensure consistency between the experimental and simulated results.

The wide variety of critical defects that are manifested in modern fabrication processes makes it necessary for the simulation tools to have the ability to rigorously model size, shape and material of the wafer topography. Additionally, to optimize detection ability, parameters such as wavelength, numerical aperture, and polarization of light must be investigated. METRO 3-D is a simulation program that solves the rigorous three dimensional Maxwell's equations and provides the flexibility to model these parameters used to define in-line detection schemes.

In this paper the extensions and enhancements to METRO 3-D are discussed. In particular the enhancement to the simulator that allows absorbing materials to be investigated is presented. Then cases are shown that utilize METRO 3-D to illustrate the simulators ability to characterize detection schemes.

II. SIMULATION METHODOLOGY

A. Previous Work

The waveguide model used in METRO is a numerical model that calculates the reflected and transmitted electromagnetic waves from an illuminated structure. The model has been used for a variety of applications (i.e. photolithography, phase shift masking, and mask alignment) and has been extended and enhanced during its use[2]. Most recently, Lucas developed a 3-D version of METRO for analyzing mask structures. This model has been extended to include the investigation of wafer topographies.

B. The 3-D Model Methodology

The flow of the simulator is separated into modules that define the light source, projection optics, scattering from the wafer surface, collection optics and detection system as in Fig.1a. To solve for the reflected light from a wafer topography, the electromagnetic field within the topography must be solved. In this method, the Maxwell Equations and the Lorentz gauge transformation are used to allow only the vector potential to be solved as in equations (1) - (3) and from these equations the scattering of light from the wafer topography can be obtained.

$$\nabla^2 A_x + k^2 \epsilon A_x - \frac{\partial}{\partial x} \log \epsilon \left(\frac{\partial A_x}{\partial x} + \frac{\partial A_y}{\partial y} \right) = 0 \quad (1)$$

$$\nabla^2 A_y + k^2 \epsilon A_y - \frac{\partial}{\partial y} \log \epsilon \left(\frac{\partial A_x}{\partial x} + \frac{\partial A_y}{\partial y} \right) = 0 \quad (2)$$

$$A_z = 0 \quad (3)$$

A is the vector potential, and ϵ is the dielectric constant of the material in the wafer topography. To obtain the waveguide equations (1) - (3), the gradient of the dielectric constant in the z direction was assumed to be zero. Therefore, to represent the wafer topography the structure is divided into discrete layers that are uniform in the vertical direction as shown in Fig. 1b.

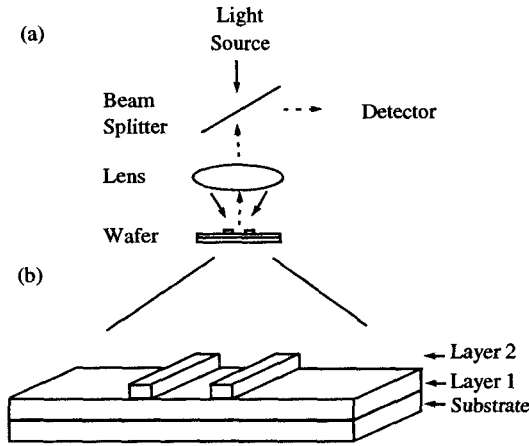


Fig. 1 (a) Bright field configuration for an in-line defect detection scheme. (b) Discretization of layers for the METRO 3-D simulator.

C. Boundary Conditions and Layer Stitching

Since the topography is discretized into layers the electromagnetic boundary conditions between the layers must be satisfied and can be solved using equations (4) - (5).

$$E_x^j = E_x^{j+1} \quad E_y^j = E_y^{j+1} \quad (4)$$

$$H_x^j = H_x^{j+1} \quad H_y^j = H_y^{j+1} \quad (5)$$

To solve for the scattering of light from the wafer topography, the electromagnetic conditions for each layer, equations (1) - (3), must be stitched to the adjacent layer by using equations (4) - (5). By stitching two adjacent layers, it provides a set of equations, known as the interface matrix, I, that couples the forward modes (C) and backward modes (C') of the two layers, as in equation (6).

$$\begin{bmatrix} C^j \\ C'^j \end{bmatrix} = I^j \begin{bmatrix} C^{j+1} \\ C'^{j+1} \end{bmatrix} \quad (6)$$

The method used in the previous model to stitch the interface matrices together was the T-matrix formulation. For T-

matrix propagation, the interface matrix is simply multiplied from one layer to the next, as shown in equation (7), to obtain the final transfer matrix, T^0 . From T^0 the reflected light amplitudes are calculated[3].

$$T^0 = I^0 \dots I^{j+1} \cdot I^{j+2} \dots I^q \quad (7)$$

One of the most challenging topographies to model is a structure containing highly absorbing material (such as metal or polysilicon), because the boundary conditions between two layers require that the forward propagating and backward propagating electromagnetic waves be calculated simultaneously. If there are a large number of evanescent waves in the calculation, or if one of the layers contains an absorbing material, the solution will contain exponentially growing and decaying modes, making it difficult to maintain numerical stability. In the previous version of METRO, the transfer matrix formulation was used to calculate the reflected and transmitted light from mask structures. With this method, numerical instability occurs for absorbing material because the forward and backward modes are subtracted. To allow for the simulation of absorbing materials, the scattering matrix (S-matrix) formulation was developed[4][5].

The S-matrix is explicitly arranged so that the forward and backward modes are combined to avert numerical instability. The scattering matrix, S^j , for a structure with n layers is defined in equation (8) where the C^j vectors contain the coefficients of the forward modes and the C'^j vectors contain the coefficients of the backward modes for layer j. The S matrix for the (j+1)th layer is given in terms of the jth layer S matrix and the interface matrix in equation (9) as four sub-matrices: S_{11} , S_{12} , S_{21} and S_{22} . This is obtained by using the boundary conditions of equation (6) and equation (8).

$$\begin{bmatrix} C^{j+1} \\ C'^{j+1} \end{bmatrix} = S^{j+1} \cdot \begin{bmatrix} C^j \\ C'^j \end{bmatrix} \quad (8)$$

$$\begin{aligned} S_{11}^{j+1} &= \left(I_{11}^j - S_{12}^j \cdot I_{21}^j \right)^{-1} S_{11}^j \\ S_{12}^{j+1} &= \left(I_{11}^j - S_{12}^j \cdot I_{21}^j \right)^{-1} \left(S_{21}^j \cdot I_{22}^j - I_{12}^j \right) \\ S_{21}^{j+1} &= S_{22}^j \cdot I_{21}^j \cdot S_{11}^{j+1} + S_{21}^j \\ S_{22}^{j+1} &= S_{22}^j \cdot I_{21}^j \cdot S_{12}^{j+1} + S_{22}^j \cdot I_{22}^j \end{aligned} \quad (9)$$

III. RESULTS

The 3-D waveguide model for simulation of wafer structures has enabled the investigation of several wafer topographies. To illustrate the ability of the simulator, two practical

examples are shown here: a case in which experimental data from AMD Sunnyvale is compared to simulation results and a general case containing metal lines so that a highly absorptive material could be studied.

A. Industrial Case

For the example shown here, contaminants were followed through a series of process steps at AMD Sunnyvale and their characteristics were extracted at each of the inspections providing a large database of contaminants that are present in a modern fabrication facility. The purpose of this case was to simulate the detection of interesting defects that are in this database. One particular case is illustrated in Fig.2, where the defect is seen by a KLA 2131 system and a SEM. The defect was captured by the KLA system after silicon nitride was etched; therefore, the defect was modeled as a silicon nitride particle. It is difficult to determine the exact location of the particle but from inspecting the KLA and SEM images it was determined to be on top of the silicon dioxide line (bright defect on dark line as in Fig.2a and Fig.3). For simulation, the optical configuration of the inspection was set up to mimic the KLA 2131 so a comparison could be made between the simulator and a detection scheme image. Although the magnification and field of view of the KLA image (Fig.2) is not on the same scale as the simulation images (Fig.3), the similarities between the simulation and the KLA result illustrate the ability of METRO 3-D to model asymmetric 3-D wafer topographies and the detection schemes that are used to capture defects. Such simulations can be used to optimize the detection schemes by changing the type of illumination and the detection optics.

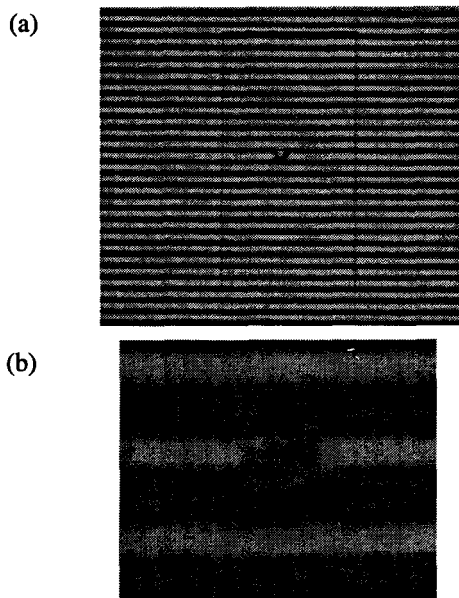


Fig. 2 Silicon nitride defect on a silicon dioxide - silicon grating as seen by: (a) KLA 2131 inspection system (b) Scanning Electron Microscope (SEM).

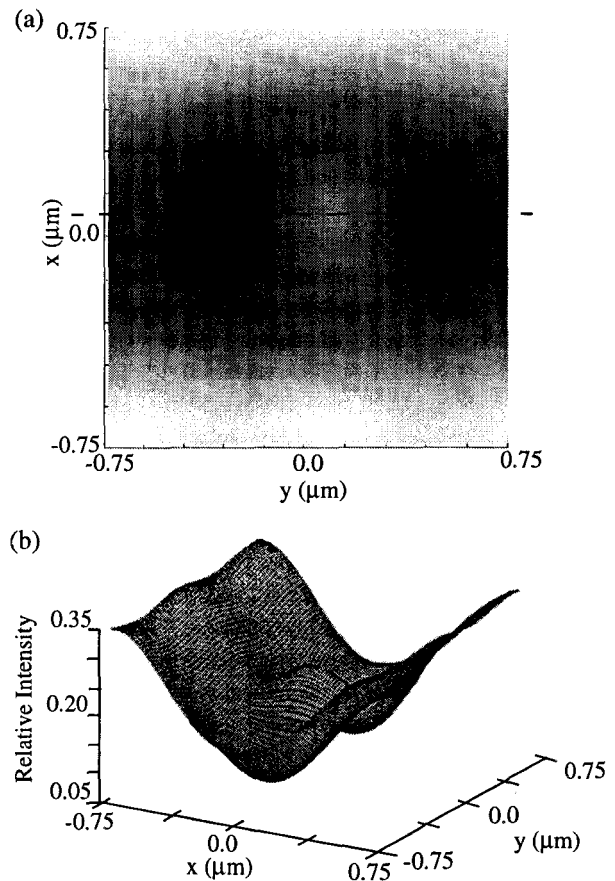


Fig. 3 Image of the silicon dioxide line with a silicon nitride defect: (a) Top view and (b) 3-D image.

B. Metal Lines

To illustrate the ability to simulate highly absorptive material, a metal line structure is considered. The topography is composed of two aluminum lines on a silicon dioxide - silicon stack. The thickness of the silicon dioxide was chosen to be one micron and the metal line thickness was chosen to be 0.6 micron. For the first case the topographies was modeled to approximate aluminum that has unnecessarily been etched from the metal line and a line break of 0.3 micron has occurred in the left line. Since the aluminum has been completely removed from a segment on the left line, this will cause an open fault in the resulting circuit.

Fig.4 and Fig.5 show the resulting bright field inspection, using numerical aperture of 0.15 and 0.45 respectively, of the aluminum lines after the lines have been defined by the etching process. The scattering of light from the area of missing aluminum is observed for both numerical apertures shown, but for the high NA scheme the defect intensity is greater

than for the lower NA scheme. Using the rigorous simulation program provides insight into the scattering of light from the highly absorptive metal without having to investigate a large number of experimental wafers.

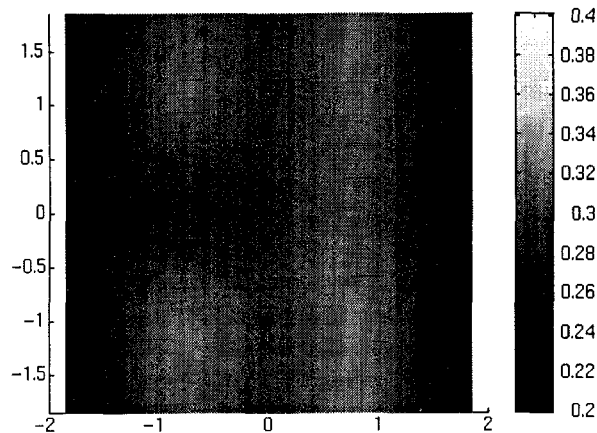


Fig. 4 Top view image of aluminum lines on a silicon dioxide - silicon stack with a line break of $0.3\mu\text{m}$ using a numerical aperture of 0.15.

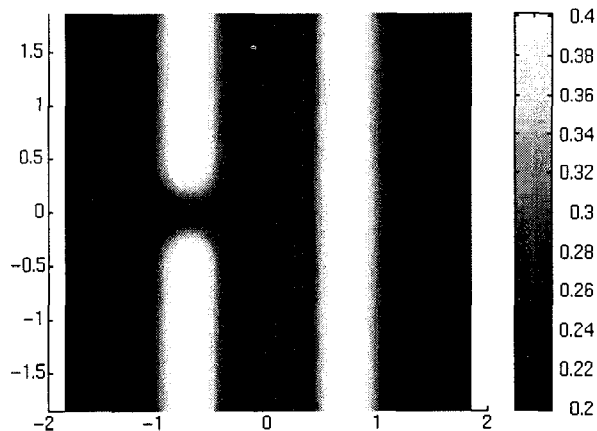


Fig. 5 Top view image of aluminum lines on a silicon dioxide - silicon stack with a line break of $0.3\mu\text{m}$ using a numerical aperture of 0.45.

After the completion of this nominal case, a study was performed to consider the effects of the size of the line break and the effect of the numerical aperture being used in the inspection scheme. Line breaks of 0.2, 0.3 and 0.5 micron and numerical apertures of 0.15, 0.30, 0.45 and 0.60 were investigated. As expected, as the size of the defect increased and as the numerical aperture increased so did the defect intensity seen by the inspection system. Additionally, it can be seen that for the 0.3 micron defect size, the affect of using a higher numerical aperture is not a linear increase.

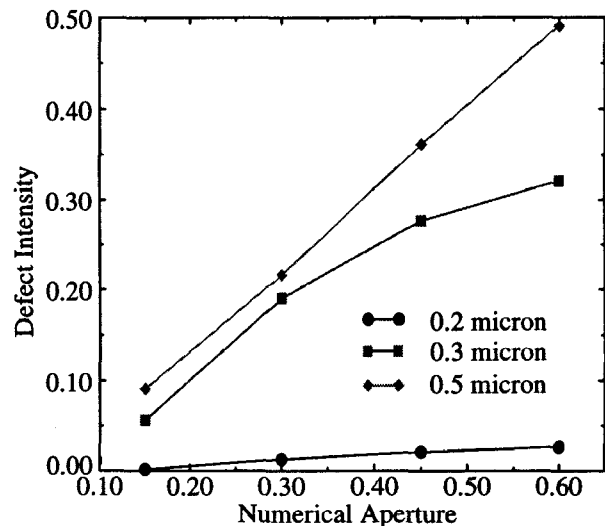


Fig. 6 Defect intensity versus numerical aperture for a aluminum lines with defect of sizes 0.2, 0.3 and 0.5 μm .

IV. CONCLUSION

A rigorous 3-D topography simulator based on the waveguide method has been developed to allow the prediction and correlation of the critical physical parameters (material, size and location). The model has been enhanced to be capable of simulating the effects of light scattering on highly absorptive materials in the VLSI manufacturing process. The simulation of defect examples using METRO 3-D was compared with data gathered from the AMD-Sunnyvale fab line. A good match was obtained indicating the accuracy of this method which provides a framework for characterization of in-line defect detection schemes for modern semiconductor manufacturing.

ACKNOWLEDGMENT

This work is supported by SRC, Pennsylvania Sematech Center Of Excellence for Rapid Yield Learning under contract MC-511.

REFERENCES

- [1] A. Swecker, A. Strojwas, A. Levy, B. Bell, "Comparison of Defect Detection Schemes Using Rigorous 3-D EM Field Simulations," *SPIE* 1997.
- [2] C. Yuan, *Modeling of Optical Alignment and Metrology in VLSI Manufacturing*, Ph.D. Dissertation, Carnegie Mellon University, 1989.
- [3] K. Lucas, A. Strojwas, H. Tanabe, "Efficient and Rigorous 3D Model for Optical Lithography Simulation," *J. Opt. Soc. Am. A*, Vol.13, No.11 Nov. 1996; pp. 2187-99.
- [4] D. Ko, J. Sambles, "Scattering Matrix Method for Propagation of Radiation in Stratified Media: Attenuated Total Reflection Studies of Liquid Crystals," *J. Opt. Soc. Am. A*, Vol. 5 No. 11, pp. 1863-1866, Nov. 1988.
- [5] L. Li, C. Haggans, "Convergence of the Coupled-Wave Method for Metallic Lamellar Diffraction Gratings," *J. Opt. Soc. Am. A*, Vol. 10 No. 6, pp. 1184-1189, June 1993.